Environ Fluid Mech (2009) 9:369–387
DOI 10.1007/s10652-008-9105-4

ORIGINAL ARTICLE

Mass-based depth and velocity scales for gravity currents and related flows

M. Princevac · J. Bühler · A. J. Schleiss

Received: 16 August 2008 / Accepted: 23 September 2008 / Published online: 12 October 2008

Abstract Gravity driven flows on inclines can be caused by cold, saline or turbid inflows into water bodies. Another example are cold downslope winds, which are caused by cooling of the atmosphere at the lower boundary. In a well-known contribution, Ellison and Turner (ET) investigated such flows by making use of earlier work on free shear flows by Morton, Taylor and Turner (MTT). Their entrainment relation is compared here with a spread relation based on a diffusion model for jets by Prandtl. This diffusion approach is suitable for forced plumes on an incline, but only when the channel topography is uniform, and the flow remains supercritical. A second aspect considered here is that the structure of ET's entrainment relation, and their shallow water equations, agrees with the one for open channel flows, but their depth and velocity scales are those for free shear flows, and derived from the velocity field. Conversely, the depth of an open channel flow is the vertical extent of the excess mass of the liquid phase, and the average velocity is the (known) discharge divided by the depth. As an alternative to ET's parameterization, two sets of flow scales similar to those of open channel flows are outlined for gravity currents in unstratified environments. The common feature of the two sets is that the velocity scale is derived by dividing the buoyancy flux by the excess pressure at the bottom. The difference between them is the way the volume flux is accounted for, which—unlike in open channel flows—generally increases in the streamwise direction. The relations between the three sets of scales are established here for gravity currents by allowing for a constant co-flow in the upper layer. The actual ratios of the three width, velocity, and buoyancy scales are evaluated from available experimental data on gravity currents,

M. Princevac
Department of Mechanical Engineering, University of California at Riverside, Bourns Hall A315, Riverside, CA 92521, USA
e-mail: marko@engr.ucr.edu

J. Bühler (✉)
Institute of Environmental Engineering, ETH Zurich, 8093 Zurich, Switzerland
e-mail: buhler@ifu.baug.ethz.ch

A. J. Schleiss
Ecole Polytechnique Fédérale de Lausanne, Laboratory of Hydraulic Constructions, Station 18, 1015 Lausanne, Switzerland
e-mail: anton.schleiss@epfl.ch

and from field data on katabatic winds. A corresponding study for free shear flows is referred to. Finally, a comparison of mass-based scales with a number of other flow scales is carried out for available data on a two-layer flow over an obstacle. Mass-based flow scales can also be used for other types of flows, such as self-aerated flows on spillways, water jets in air, or bubble plumes.

Keywords Top-hat scales · Flow scales · Gravity currents · Two-layer flow · Entrainment · Katabatic winds

1 Introduction

The width and velocity of nonbuoyant jets and wakes has traditionally been specified in terms of the maximum velocity anomaly u_{em} at the center of the flow, and the half-width b_u at which the anomaly decays to one-half of the maximum value. Both of these scales are thus based on local properties of the velocity distribution. By invoking the concept of self-preservation, velocity distributions were computed on the basis of the mixing length, eddy viscosity, and related concepts. The predictions were compared with measured distributions, often with little concern about the agreement of predicted and measured fluxes of volume and momentum. A diffusion model for the streamwise widening rate of such flows was proposed by Prandtl [1] (see also [2,3]). His basic concept is that the outward drift of turbulent structures advected downstream with the main flow is proportional to their excess velocity relative to the ambient fluid, which implies that Db_u/Dt is proportional to u_{em}. For jet-like flows in calm ambients u_{em} is the maximum velocity u_m, and with $Db_u/Dt = \mathrm{d}b_u/\mathrm{d}x u_m$, this leads to $\mathrm{d}b_u/\mathrm{d}x = \text{const}$. Whenever needed, the half-width b_c of the distribution of a passive tracer, or of a stratifying agent in buoyant plumes, was related to the velocity half-width as $b_c = \lambda b_u$, with λ being a coefficient of proportionality. When the velocity distribution is determined from experiments only, the resulting fluxes of volume and momentum can be related to the two local flow scales by integration constants [4].

A different type of flow scales, derived from integrals over the velocity distribution, has been used for boundary layers, which lack in self-preservation. Examples are the displacement and momentum thicknesses. The main feature of these flow scales is that the integration over the velocity distribution is carried to a region outside the boundary layer, where the shear stress vanishes. Their advantage is that they do not hinge on a particular shape of the profiles, and thus provide an additional basis for comparisons of different experiments, even for self-preserving flows. Another set of such flow scales are the ones proposed by Morton, Taylor and Turner [5] (MTT), who studied jets and plumes by allowing for the presence of an ambient stratification. Flows in stratified surroundings lack in self-similarity as well, and the scales for width and velocity were derived from the fluxes of volume and momentum instead of using local flow scales. Similarly, the buoyancy scale was based on the buoyancy flux. To simplify previous analyses they also assumed Gaussian distributions of velocity and buoyancy. The variation of the fluxes of volume and buoyancy was accounted for by introducing the entrainment principle, which implies that the velocity of ambient fluid flowing through the boundary of the flow is proportional to the average streamwise velocity. The constant of proportionality is called the entrainment constant.

The entrainment constants were compared with the widening rates for steady jet-like flows [6–9], as well as for thermals and puffs, for which the diffusion and entrainment approaches are consistent with each other [10]. For calm and unstratified ambient fluids, both of these models predict a constant spatial widening rate for all of these flows. The main difference

is that the widening rates can be derived from the diffusion model without making use of the momentum equation. Unlike the entrainment constants, these rates also agree quite well for nonbuoyant and buoyant flows on one hand, and for plane and axisymmetric shear flows on the other [11]. We noticed that the origin of the diffusion approach appears to be getting lost, Patel [4] already referred to Abramovich [3] as attributing it to Prandtl. In this study we show that the diffusion model is particularly suitable for forced plumes flowing down an incline. In the aquatic environment such flows can arise when the flow is released into an aquifer under some pressure to enhance dilution.

Ellison and Turner [12] (ET) applied the MTT approach to gravity currents in deep water, which generally also lack in self-preservation due to changes in slope and bottom roughness. An entrainment function which depends on the Richardson number of the flow then replaces the entrainment constant, and two shape factors, S_1 and S_2, are required to relate the top-hat scales to gravitational terms in the momentum equation. The ET approach has been used to describe gravity and turbidity currents in lakes and marine environments [13–17]. Manins and Sawford [18] used them for a field study on katabatic (downslope) winds in a stratified atmosphere. Numerical predictions are required for more complex topographies, stratified environments, and gravity currents impeded by obstacles. Numerical simulations are especially useful when supported by field or laboratory data [19,20].

Ellison and Turner noted that their shallow water equations for gravity currents agree with the Bresse equations for open channel flows. Whereas the structure of the two sets is indeed the same, their depth and velocity scales are those of MTT for free shear flows. The two types of scales differ because the width of free shear flows is derived from the velocity distribution, whereas the depth h of open channel flows is the vertical extent of the excess mass of the liquid phase. This extent can be determined visually, or by means of floats. Floats are supported by the jump in density across this interface, which represents a local property of the vertical density distribution. Since the liquid density ρ is constant, and having g as the gravitational acceleration, the depth can also be determined from the excess pressure $\rho g h$ at the bottom, or from the excess pressure force $\rho g h^2/2$, which reflect integral properties of the density distribution. When there are no lateral inflows, the discharge is conserved, and the mean velocity is the discharge divided by the depth. A slightly different picture emerges when open channel flows are considered as a special case of two-layer flows. In this view the buoyancy flux $\rho g u h$ in the liquid layer is conserved, and the mean velocity u is the buoyancy flux divided by the excess pressure at the bottom. For normal flows the velocity distribution remains self-preserving, and the momentum flux is related to the velocity and depth scales by a shape factor, the momentum coefficient β, which accounts for the nonuniformity of the velocity distribution.

To reconcile the approaches for free shear flows, gravity currents, and open channel flows, the same mass-based velocity scale u can also be used for all of them. In contrast to open channel flows, however, the distribution of excess density in gravity currents is generally not uniform across their depth. As a consequence, both the excess flow force and the excess bottom pressure have to be determined to derive scales for the mean buoyancy g' and the depth h of the flow. Unlike in open channel flows, the volume flux in gravity current generally increases in the flow direction. This requires an additional shape coefficient γ, which accommodates this flux, and thus distinguishes the extent h of the excess mass, from the total depth γh of moving fluid. Finally, the momentum flux is accounted for by modifying the streamwise velocity by a momentum coefficient analogous to the one for open channel flows. The corresponding mass-based flow scales and shape factors were derived by Buhler and Schlaepfer [21].

Noh and Fernando [22] proposed scales which are intermediate between those of ET and fully mass-based ones. They also derived the flow velocity from the buoyancy flux and the bottom pressure, but retained the volume flux to determine their only depth scale, which corresponds to γh.

In Sect. 2 of the present contribution, ET's shallow water equations are outlined by considering the presence of ambient co-flows in the upper layer, and their entrainment relation is compared with a diffusion model by Bühler et al. [9]. In Sect. 3 the limitations of the ET scales are illustrated, and their relation with the two sets of mass-based flow scales is established for gravity currents in co-flowing ambient fluids. To illustrate the difference between the three parameterizations, corresponding values of the scales, and shape factors, are evaluated from available laboratory data on gravity currents and free shear flows in Sect. 4. Field data on katabatic winds of Princevac et al. [23] are evaluated in the same way in Sect. 5, followed by laboratory data on two-layer flows over an obstacle in Sect. 6. Conclusions are drawn in the final section.

2 Velocity-based width scales for free shear flows and gravity currents

In this section traditional flow scales for self-preserving jet-like flows are outlined, and the top-hat flow scales of ET are examined for gravity currents in co-flows, sketched in Fig. 1. The motivation for including co-flows was provided by a study on katabatic winds in October 2000, the Vertical Transport and Mixing Experiment (VTMX) in Salt Lake City [23]. By invoking the boundary layer approximations, the excess momentum of a gravity current in a co-flow of velocity u_a can be stated as

$$\frac{\mathrm{d}}{\mathrm{d}x}\left[\int \bar{u}(\overline{\rho u}-\rho_a u_a)\mathrm{d}y + g\cos\varphi\int(\overline{\rho}-\rho_a)\,y\mathrm{d}y\right] = -\frac{\mathrm{d}(\rho_a u_a)}{\mathrm{d}x}\left(\int(\overline{u}-u_a)\,\mathrm{d}y + u_a h_a\right) + g\sin\varphi\int(\overline{\rho}-\rho_a)\mathrm{d}y - \tau_b \qquad (1)$$

and buoyancy is conserved when

$$g\frac{\mathrm{d}}{\mathrm{d}x}\int\left((\overline{\rho}-\rho_a)\,\overline{u}+\overline{\rho' u'}\right)\mathrm{d}y = 0. \qquad (2)$$

The index a refers to the ambient (i.e. upper) layer, which is considered as being unbounded and unstratified, x and y are the streamwise and transverse coordinates, and φ is the slope angle. The mean local density $\overline{\rho}$ is often determined by relating it to the concentration $\overline{c}$ of the stratifying agent, and $\overline{u}$ is the mean local velocity. The turbulent contribution $\overline{\rho' u'}$ to the buoyancy flux is included here, as this flux is generally the only one which can be truly conserved, τ_b is the shear stress at the bottom, and h_a is a depth scale to be determined. The contribution of the excess mass to the momentum flux is accounted for to retain the connection with open channel flows. The integration is carried from the bottom to some level in the uniform ambient layer at which $\mathrm{d}\overline{u}/\mathrm{d}y$, the excess density, and the corresponding fluctuations, can be neglected.

The two equations can also be applied to free jets and plumes, for which the shear stress at the center plane $y = 0$ vanish. For these flows the traditional approach for simplifying (1) and (2) is then to express the integrals in terms of the maximum excess velocity u_{em} and the jet half-width b_u, by assuming the profiles to be self-preserving, i.e. geometrically similar. A shape function for the velocity profiles, such as a Gaussian, and a closure relation for the widening rate are then required.

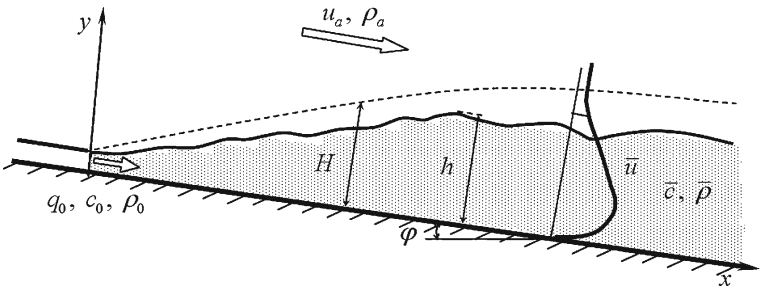

Fig. 1 Definition sketch for a gravity currents emerging from a duct into unstratified and deep water. Depth scales H and h are based on the distributions of velocity $\bar{u}$ and excess mass $\bar{\rho} - \rho_a$, respectively, $\bar{c}$ is the concentration of the stratifying agent; q_0 the initial discharge per unit width. Subscript a refers to the ambient values

Gravity currents are generally not self-preserving due to changes in topography, and ET used MTT's concept to describe them. By including the case of ambient co-flows, they represented the integrals in (1) in terms of top-hat scales for the depth H, the excess velocity U according to

$$UH = \int (\overline{u} - u_a)\mathrm{d}y \tag{3}$$

$$U^2 H = \int (\overline{u} - u_a)^2 \mathrm{d}y \tag{4}$$

A buoyancy scale Δ was derived from the buoyancy flux specified in (2) as

$$(U + u_a)\Delta H = g \int \frac{(\overline{\rho} - \rho_a)\,\overline{u} + \overline{\rho' u'}}{\rho_a} \mathrm{d}y = \Delta_0 q_0 \tag{5}$$

where q_0 is the source flow rate and Δ_0 is the buoyancy at the source. ET neglected the turbulent flux in their formulation, but in their experiments they also determined Δ by dividing the known buoyancy flux at the source by the measured volume flux.

To account for the effect of the slope angle and ambient velocity, they modified the entrainment approach of MTT by proposing an entrainment relation of the form

$$\frac{\mathrm{d}}{\mathrm{d}x}[(U + u_a)H] = EU, \tag{6}$$

where $E(Ri_e)$ is an entrainment function which depends on the Richardson number $Ri_e = \Delta H \cos\varphi / U^2$.

After dividing them by ρ_a, the momentum and buoyancy equations (1) and (2) can then be restated for dilute flows as

$$\frac{\mathrm{d}}{\mathrm{d}x}\left[U(U + u_a)H + \frac{S_1}{2}\Delta H^2 \cos\varphi\right] = -\frac{\mathrm{d}u_a}{\mathrm{d}x}(U + u_a)H + S_2 \Delta H \sin\varphi - C_D(u_a + U)^2 \tag{7}$$

and

$$\frac{\mathrm{d}}{\mathrm{d}x}[\Delta(U + u_a)H] = 0. \tag{8}$$

By following ET, the bottom shear stress is expressed in terms of a Chezy-type drag coefficient C_D, and the depth h_a, which determines the contribution $u_a h_a$ of the ambient flow to the volume flux in (1), is set equal to H in (6), (7) and (8). The contribution of the ambient flow to the flux of volume, and to the buoyancy Δ, thus depend on this definition of h_a, whereas the contribution to the momentum flux vanishes when $\mathrm{d}u_a/\mathrm{d}x = 0$. Wright [24] used the corresponding approach for axisymmetric jets in co-flows.

The shape factors S_1 and S_2 of ET relate the excess bottom pressure and the excess pressure force to the flow scales, i.e.

$$S_1 \Delta H^2 = 2g \int \frac{(\overline{\rho} - \rho_a)}{\rho_a} y \mathrm{d}y$$
$$S_2 \Delta H = g \int \frac{(\overline{\rho} - \rho_a)}{\rho_a} \mathrm{d}y \tag{9}$$

An important result of ET for flows with $\mathrm{d}u_a/\mathrm{d}x = 0$ is that an equilibrium state is reached at some distance from the source, in which the velocity U, as well as the Richardson number $Ri = \Delta H(U + u_a)\cos\varphi$, and $\mathrm{d}H/\mathrm{d}x$ become constant. ET also carried out a series of experiments for $u_a = 0$, and determined the entrainment function for a number of slope angles. The shape constant S_1 varied in the range from 0.2 to 0.3, S_2 from 0.6 to 0.9. They also performed experiments for a surface layer of fresh water flowing over a stagnant layer of salt water to determine the limit of approximately $Ri = 0.83$, at which the entrainment ceases. Higher limiting values up to $Ri = 23$ were found by Fernandez and Imberger [17] in field experiments. These authors also provided a survey of entrainment relations which modify the one by ET, and were proposed by later investigators.

As an estimate for the value of E for wall jets and wall plumes ($Ri = Ri_e = 0$) ET adopted a value of $E = 0.075$ for free jets [25], which corresponds to $\mathrm{d}H/\mathrm{d}x = 2E = 0.15$. They already noted that the value of E for free plumes, which would be more appropriate for buoyant flows, appeared to be higher, but thought that insufficient data were available to make definite conclusions. More recent experiments show that $E = \mathrm{d}H/\mathrm{d}x$ for free plumes is about 0.15 [11]. Results for wall jets in a uniform stream by Patel [4] indicate that $\mathrm{d}H/\mathrm{d}x = 0.091$ for these flows. Similar to what is found for free shear flows, this widening rate is again in excellent agreement with the value of $E = \mathrm{d}H/\mathrm{d}x = 0.095 \pm 0.005$ for wall plumes obtained by Grella and Faeth [26]. To account for this, Bühler et al. [9] suggested using a formulation $DH/Dt = DU$ in the spirit of Prandtl's approach, where D is a diffusion function, or

$$\frac{\mathrm{d}H}{\mathrm{d}x} = D\frac{U}{U + u_a}, \tag{10}$$

for forced plumes on an incline, and similar developing gravity currents. For equilibrium flows this relation agrees with (6) and $D(Ri_e) \equiv E(Ri_e)$. As the modifications of ET's entrainment relation by later investigators listed in [17] are also for equilibrium flows, these models for E can be used as well. The diffusion relation (10) can thus be expected to work for developing gravity currents if $D(0)$ is increased from 0.075 to about 0.093. As this relation is not consistent with the entrainment relation (6), it is limited to flows on uniform topography, i.e. when depth changes are not related to variations in slope or flow cross-section. Similar limitations related to changes in topography apply for an entrainment relation $\mathrm{d}(HU)/\mathrm{d}x = E'U$, which Princevac et al. [23] proposed for katabatic winds in co-flows. For equilibrium flows their relation reduces to $\mathrm{d}H/\mathrm{d}x = E'$.

3 Mass-based width scales for gravity currents and open-channel flows

The difference between the flow scales of ET and those for open channel flows is that they are derived from the velocity distribution, whereas the depth of flows with a free surface is the vertical extent of the excess mass. A consequence is that when the ET scales are applied to gravity currents in co-flows, the value of Δ depends on u_a according to (5). The shape factors S_1 and S_2 then also depend on u_a, instead of reflecting the nonuniformity of the excess velocity and buoyancy profiles only. These limitations can be avoided for entraining gravity currents in deep and unstratified water by noting that the integrals over the buoyancy distribution in (9) are available for replacing the fluxes of volume and momentum as a basis for deriving flow scales. The resulting scales are then associated with the distribution of excess mass and vorticity, and consistent with those for open channel flows.

A first option is to make use of (5), and both integrals in (9), and to derive all three flow scales, instead of only one, from the flux and distribution of buoyancy. This is leads to scales for velocity u, buoyancy g' and depth h given by

$$\begin{aligned} g'h &= g\int \frac{(\overline{\rho}-\rho_a)}{\rho_0}\mathrm{d}y \\ g'h^2 &= 2g\int \frac{(\overline{\rho}-\rho_a)}{\rho_0}y\mathrm{d}y \\ g'hu &= g\int \frac{(\overline{\rho}-\rho_a)\,\overline{u}+\overline{\rho' u'}}{\rho_0}\mathrm{d}y \end{aligned} \tag{11}$$

which can be used for both dilute and dense gravity currents. For open channel flows $\rho_a \to 0$, $g' = g$, and $\overline{\rho} = \rho_0$.

The excess fluxes of mass and momentum in (1) and (2) can then be specified as

$$\begin{aligned} m_e = \int (\overline{\rho u} - \rho_a u_a)\,\mathrm{d}y &= \left[\rho + (\gamma-1)\,\rho_a\right] uh - \gamma\rho_a u_a h \\ &= (\rho-\rho_a)\,uh + \gamma\rho_a\,(u-u_a)\,h, \\ M_e = \int \overline{u}\,(\overline{\rho u} - \rho_a u_a)\mathrm{d}y &= \left[\rho + (\gamma-1)\,\rho_a\right]\beta u^2 h - \gamma\rho_a u_a uh \\ &= \beta\,(\rho-\rho_a)\,u^2 h + \gamma\rho_a\,(\beta u - u_a)\,uh \end{aligned} \tag{12}$$

The velocity scale u in this parameterization of m_e is associated both with the mass flux ρuh of the dense layer of depth h, as well as with the flux of ambient fluid in a superimposed layer of depth $(\gamma-1)h$. As we shall see, the total depth γh generally exceeds h in gravity currents. The purpose of γ is similar to that of the turbulent Schmidt number, $1/\lambda$, in free shear flows. The present approach is also related to the one for thermals and puffs, the extent of which has been determined by means of flow visualization. The factor $(\gamma-1)$ corresponds to the virtual mass coefficient of these unsteady flows, and accounts for the momentum associated with ambient fluid [27].

The excess momentum flux in (12) is accounted for by modifying the square of the flow velocity by a single momentum coefficient β, which was introduced by Boussinesq [28] for open channel flows. The terms in ρ_a, which are associated with the excess mass flux in the gaseous upper layer, can be neglected for these flows. The momentum coefficient β is also used for flows in ducts, and accounts for the nonuniformity of the velocity profile. It ranges from 1.03 to 1.33 in open channel flows; the values for a linear laminar profile are 1.33, and 1.2 for a parabolic one [29]. The corresponding ET scales would be $H = h/\beta$, $U = \beta u$, and can thus differ considerably from the depth h and the mean velocity u of the liquid layer.

For dilute flows, the remaining integrals in (1) and (2) can be expressed as

$$\frac{\mathrm{d}}{\mathrm{d}x}\left[\gamma(\beta u - u_a)uh + \frac{1}{2}g'h^2\cos\varphi\right] = -\frac{\mathrm{d}u_a}{\mathrm{d}x}\gamma uh + g'h\sin\varphi - C_D^* u^2 \tag{13}$$

and

$$\frac{\mathrm{d}}{\mathrm{d}x}(g'uh) = 0. \tag{14}$$

The star in C_D^* denotes definitions in terms of mass-based scales. An analogous approach can be used for the energy equation of gravity currents [30], which leads to an energy coefficient similar to the Coriolis coefficient for open channel flows [29].

The scales, and the shape factors for dilute flows are related to those of ET by

$$\begin{aligned} g'h^2 = S_1\Delta H^2, \quad g'h = S_2\Delta H, \quad g'hu = \Delta(U+u_a)H \\ \gamma(u-u_a)h = UH, \quad \gamma(\beta u - u_a)uh = U(U+u_a)H \end{aligned} \tag{15}$$

and a continuity equation patterned after (6) is

$$\frac{\mathrm{d}}{\mathrm{d}x}(hu) = E^* u_e \tag{16}$$

where $u_e = u - u_a$. The entrainment function $E^*(Ri_e^*)$ is related to $Ri_e^* = g'h\cos\varphi/(u-u_a)^2$. Note that the entrainment rate is stated in terms of the depth h and velocity u associated with the flux and distribution of buoyancy. As a consequence, E^* can be determined based on density measurements alone according to (11) when this flux, and u_a, are known. Equation (16) also reduces to the continuity equation for open channel flows when E^* vanishes. Equations (6), (7), and (8) can then be stated in terms of mass-based scales as

$$\frac{\mathrm{d}h}{\mathrm{d}x} = \frac{E^*(1-u_r)\left(\gamma(2\beta - u_r) - \frac{1}{2}Ri^*\right) - Ri^*\tan\varphi + C_D^*}{\beta\gamma - Ri^*} \tag{17}$$

$$\frac{h}{3Ri^*}\frac{\mathrm{d}Ri^*}{\mathrm{d}x} = \frac{E^*(1-u_r)\left(\gamma(\beta - u_r) + \frac{1}{2}Ri^*\right) - Ri^*\tan\varphi + C_D^*}{\beta\gamma - Ri^*} \tag{18}$$

where $Ri^* = g_0' q_0\cos\varphi/u^3$, $u_r = u_a/u = u_a\left(Ri^*/g_0' q_0\cos\varphi\right)^{1/3}$, and $Ri_e^* = Ri^*/(1-u_r)^2$. The above equations are written in terms of Ri^* to facilitate comparisons with ET's parameterization; another suitable option for co-flows is to normalize u_a, u, and u_e with the cube root of the buoyancy flux.

The structure of (17) and (18) is the same as that of the corresponding relations derived by ET, except that their shape factors S_1 and S_2 modify Ri and $Ri\tan\varphi$, respectively, and that the velocity ratio u_r was zero in the case they examined. For deep ambient layers the interfacial long wave speed is related to the Richardson number $Ri^* = g'h\cos\varphi/u^2$ based on the velocity u relative to the solid boundary, and it does not depend on u_a. With the present definition of β and γ the denominator in (18) then vanishes when the flow is critical, as it does in open channel flows. ET obtained the corresponding result by using the shape factor S_1 to relate the pressure force, and Ri, to their velocity-based flow scales. Conversely, it can be shown by writing (18) in terms of the ET scales, and by making use of the diffusion function (10) instead of (6), the denominator vanishes at Ri close to 4 for $u_a = 0$ [9]. This is again due to the fact that (10) is not a continuity equation. The same holds when mass-based scales are used. The corresponding parameterizations can thus be expected to hold for developing flows on uniform topography only, and when the resulting equilibrium flow remains supercritical.

The relation between the flow parameters of ET and those for mass-based scales can be obtained from (15) as

$$\begin{aligned} &h = \tfrac{S_1}{S_2} H, \quad g' = \tfrac{S_2^2}{S_1} \Delta, \quad u = \tfrac{U+u_a}{S_2}, \quad u_e = \tfrac{U+u_a(1-S_2)}{S_2} \\ &\beta = S_2 \left(1 + \tfrac{u_a(1-S_2)}{U+u_a}\right), \quad \gamma = \tfrac{S_2^2}{S_1} \tfrac{U}{U+u_a(1-S_2)} \\ &E^* = E \tfrac{S_1}{S_2} \tfrac{U}{U+u_a(1-S_2)}, \quad Ri_e^* = Ri_e S_2^3 \tfrac{U^2}{(U+u_a(1-S_2))^2} \\ &Ri^* = S_2^3 Ri \end{aligned} \tag{19}$$

The values of the shape factors reported by ET for their experiments in calm water allow for a first physical interpretation of the above relations. The ranges are given as $0.2 < S_1 < 0.3$, and $0.6 < S_2 < 0.9$. The first one of relations (19) then indicates that H is larger than h for gravity currents, as sketched in Fig. 1. As a consequence, the buoyancy g' exceeds Δ, and $u > U$. The momentum coefficient β appears to be smaller than unity, whereas it is slightly larger than one in free surface and ducted flows [29]. The shape factor γ exceeds unity in gravity currents because the vertical diffusion of buoyancy within the layer is hindered by gravity.

An advantage of mass-based scales is that it is easier to determine the distribution of buoyancy, a scalar, than the velocity field. Fully mass-based scales are especially useful when the buoyancy flux is known, and conserved, as g', h, and u can then be determined from density measurements alone by making use of (11); [31]. This is possible regardless of whether an ambient flow is present or not. When u_a is known, this also holds for the determination of the entrainment function E^* in (16). Conversely, the determination of the velocity-based scales in jet-like flows, even in calm ambient fluids, is often hampered by induced flows with a streamwise component [32]. Another aspect is that the momentum flux is nonlinear in the velocity, and contains turbulent quantities as well as a pressure anomaly, which are often ignored. In view of these uncertainties it seems preferable to account for the momentum flux by a shape coefficient instead of deriving flow scales from it. The problems related to the velocity measurements then affect the shape coefficients β and γ in the momentum Eq. (13), but not the determination of the flow scales and of the entrainment function E^*. A further advantage of mass-based flow scales is that the shape factor γ allows for a geometrical interpretation, and the value of β for comparisons with open channel and ducted flows, whereas S_1 and S_2 are not easily interpretable.

The most significant difference between the flow scales of ET, and fully mass-based ones is the one between g' and Δ, as specified by the second relation in (19). Whereas g' is determined from the two moments of the transverse buoyancy distribution, the buoyancy Δ in (5) is obtained by dividing the flux of buoyancy by the volume flux. In line with this procedure, Δ_0/Δ or $(U + u_a)H/q_0$ is called the average dilution. The concept of dilution has been widely used for studies dealing with the fate of pollutants discharged into the atmosphere or surface waters. This difference between velocity and mass-based scales is especially relevant in the presence of co-flows. As mentioned earlier, the contribution $u_a H$ of the ambient flow to the volume flux in (6), and to the dilution, depends on the definition of H. ET's experimental results, for example, indicate that H is larger than the corresponding total flow depth, as $\gamma h = S_2 H$. In terms of the present scales this flux is $\gamma u_a h$, but it is unrelated to g', and the "dilution" $g_0'/g' = hu/q_0$, which is derived from the distribution of buoyancy alone. Specifically, the determination of g' neither depends on the velocity distribution, nor on whether ambient flows are present. For ET's gravity currents g' is considerably larger than Δ. The difference between the two scales can be important when the stratifying agent contains a pollutant.

A related set of top-hat scales which is also consistent with those of open channel flows was proposed by Noh and Fernando [22]; (NF). They retained ET's volume flux as a basis of their set, and only used the excess bottom pressure in (9) to replace the momentum flux. In analogy to the approach by ET, their buoyancy scale is also derived by dividing the buoyancy flux by the flux of volume, and is thus consistent with the concept of dilution. As their set is intermediate between the one of ET and fully mass-based scales, it will be denoted by the index i. In the spirit of their approach, the excess fluxes of momentum and mass for dense gravity currents in co-flows can be expressed as

$$\begin{aligned} m_e = \int (\overline{\rho u} - \rho_a u_a) \mathrm{d}y &= (\rho_i u_i - \rho_a u_a)\, h_i \\ &= (\rho_i - \rho_a)\, u_i h_i + \rho_a\, (u_i - u_a)\, h_i, \\ M_e = \int \overline{u}\, (\overline{\rho u} - \rho_a u_a) \mathrm{d}y &= (\beta_i \rho_i u_i - \rho_a u_a)\, u_i h_i \\ &= \beta_i\, (\rho_i - \rho_a)\, u_i^2 h_i + \rho_a\, (\beta_i u_i - u_a)\, u_i h_i \end{aligned} \tag{20}$$

For open channel flows the terms in ρ_a can again be neglected, so that ρ_i, u_i, and h_i correspond to the conventional scales ρ, u, and h; β_i again corresponds to the Boussinesq coefficient. For gravity currents the relations between the two sets of scales can be obtained by comparing individual terms in (12) and (20). For dilute flows they are

$$\begin{array}{llll} h_i = \gamma h, & g_i' = g'/\gamma, & u_i = u, & \beta_i = \beta \\ Ri_i = Ri, & Ri_{ie} = Ri_e^*, & E_i = \gamma E^* & \end{array}. \tag{21}$$

The flow velocity thus corresponds to u, and the shape factors β and γ again account for the excess fluxes of momentum and volume, but these authors distinguish only the single depth scale $h_i = \gamma h$. The buoyancy g', which was confined to a depth h, is thus spread out uniformly over the entire depth h_i, such that $g_i' h_i = g' h$. Equations (17) and (18) are then also valid in terms of the NF scales, when h on the LHS is replaced by h_i/γ, and E^* by E_i/γ.

4 Experimental results for gravity currents and free shear flows

Altinakar [33] determined mass-based scales, as well as those of ET for a series of experiments on saline gravity currents and turbidity currents in a 0.5 m wide channel with a test section of 12 m length. For the 12 experiments on gravity currents the slope angle φ was varied between 0.6° and 1.9°, and the buoyancy flux ranged from 0.82 to $3.09 \cdot 10^{-4} \mathrm{m}^3/\mathrm{s}^3$. At a station 4 m from the source S_1 varied from 0.48 to 1.11, $S_2 = \beta$ from 0.92 to 1.11, and Ri from 0.23 to 0.79 for all but one experiment (Salt 10). These values of β are similar to those in ducts or open channels from which gravity currents often enter a water body (Fig. 1). The corresponding range of γ was between 1.10 and 1.86, and the one of Ri^* between 0.19 and 0.68.

This author also presented figures showing the velocity and density distribution at 2, 4 and 8 m downstream from the source. They differed only slightly when they were normalized with the scales according to ET, but more significantly when mass-based scales h, u, and g' were used instead. A significant difference to ET's scales is, however, that the total depth γh of the excess motion can be distinguished from the depth h of the buoyancy distribution. Considering that the value of γ can increase from a value of one at the source, to 1.86 further downstream, a better fit might be expected by making the velocities dimensionless with γh.

This streamwise variation of γ is an example for the general lack of self-preservation of such flows. One reason is that the water depth is often limited. Another problem can be that the length of the test section is insufficient, especially when the slope, and the entrainment are small. Parker et al. [13] recommended values of 0.99 and 1 for S_1 and S_2, respectively, to obtain estimates for the evolution of gravity currents, but a rather wide range of values for S_1 and S_2 have been reported by other authors. Determinations of the shape factor γ, which allows for a geometrical interpretation, and of β, which can be compared with the momentum coefficient in open channel flows, will hopefully help to shed some more light on the picture.

Fully mass-based and intermediate top-hat scales can also be used for free axisymmetric plumes. For nonbuoyant jets the scales can be derived from the concentration $\overline{c}$ and the flux $c_o q_0$ of a passive tracer contained in the discharge, although they no longer reflect gravity forces. The spreading rates, and the decay rates for velocity and concentration for these jet-like flows can be converted into the corresponding values for mass-based scales [34]. A noteworthy result from recent sources is that the ratio γ of the total width of flow, and the extent of the excess mass or tracer carried along in it, is between 0.96 and 0.99 for plane and axisymmetric jets and plumes. This value is quite different from the ratio $1/\lambda$ of the corresponding half widths of about 0.77 for these flows. The good agreement of the lateral extent h of the buoyancy or tracer distribution with the entraining interface at $h_i = \gamma h$ also implies that both fully mass-based and intermediate flow scales are consistent with the concept of dilution. It also provides a basis for the use of a passive tracer to determine mass-based flow scales, and the dilution, along free shear flows in stratified environments. The intermediate NF scales could be applied to determine the dilution in corresponding experiments on gravity currents.

A further application of mass-based scales could be the determination of the depth h, velocity u and mean density ρ in aerated spillways. Such flows were examined by Wood [35], and the scales could be obtained from the discharge of water, and from pressure measurements on a sidewall as well as on the bottom of the channel. Analogous scales could be derived from the discharge and the concentration distribution of the dispersed phase in bubble plumes or water jets in air. The corresponding scales in the continuous phase can be obtained by adding some dye to it near the source of the flow.

5 Field observations

To provide another example for the relation between the top hat scales of ET, outlined in Sect. 2, and the two mass-based sets in Sect. 3, they were determined from field data on katabatic winds on the slope of a mountain in Utah. The data were obtained by a tethersonde system deployed during the Vertical Transport and Mixing Experiment (VTMX) sponsored by US Department of Energy. Details of the field campaign are given in Doran et al. [36]. Data collected by the Pacific Northwest National laboratory (PNNL) team at the Slope Site was used. The Slope Site is characterized by a gentle ($\varphi = 1.58°$) and very smooth (aerodynamic roughness length $\sim$0.1 m) slope. Typical measured profiles of wind speed and potential temperature (density) are shown in Fig. 2.

The profiles of wind speed and potential temperature show that the excess density distributions obtained at different times are less contorted and more consistent with each other than the corresponding velocity profiles, which have an inversion point and are strongly influenced by the no-slip condition at the bottom. This indicates that the density distribution could be a

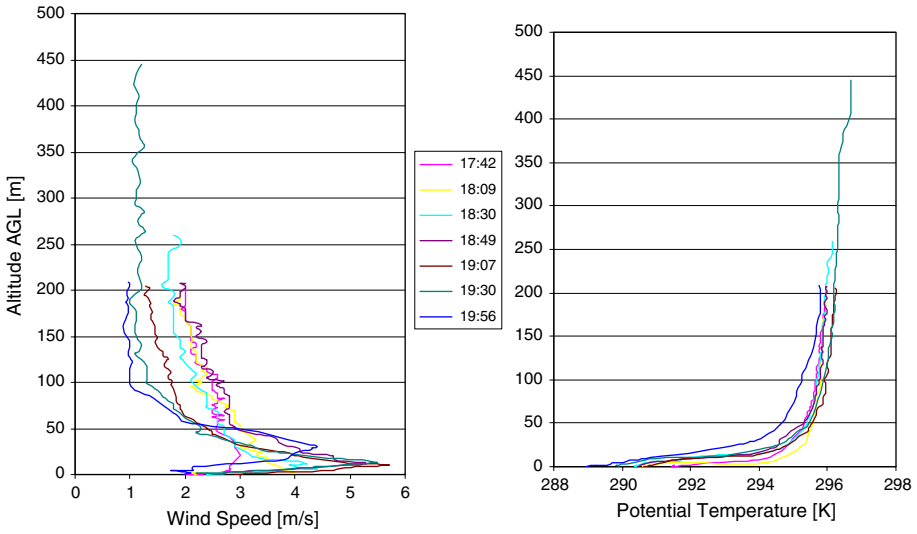

Fig. 2 Distribution of wind speed and potential temperature in katabatic winds down a slope, at different times. Heights are above ground level (from Princevac et al. [23])

more reliable basis for deriving flow scales than the velocity distribution. Apart from what looks like a small residual ambient stratification in the ascent to 450 m, the reference density in the upper layer is also more easily estimated than u_a. The range of the resulting scales and shape factors were computed by setting the integration limit at 200 m in all cases to minimize the remaining shear at the upper boundary. Turbulent fluctuations of velocity and density were not determined, and the corresponding contribution to the buoyancy flux could not be included. The results are listed in Table 1.

A comparison of the flow depths in the first three columns shows that $h < H < h_i$. The fact that H/h exceeds unity also agrees with ET's results, and with the greater width of the velocity distributions in Fig. 2. As can be expected, the corresponding buoyancy scales follow the opposite trend, i.e. $g' > \Delta > g'_i$. As mentioned earlier, the fact that the mean value of g' is almost twice as large as that of Δ and g'_i can be especially relevant in case the stratifying agent contains a pollutant. The flows are supercritical (including the one with $Ri^* = 1.20$, as $\beta\gamma = 1.23$ for this case), and the entrainment is small, as Ri_e and Ri_e^* are generally larger than the limit of $Ri_e = 0.83$ established by ET. It should be noted, however, that the entrainment relation E of ET was determined for calm upper layers; Princevac et al. [23] evaluated the entrainment rates for these field data and found higher values. Work is underway to determine the corresponding rates for mass-based flow scales. The shape factors S_1 and S_2 are somewhat higher than those measured by ET. The factor β is within the range of the momentum coefficient in open channel flows, and it agrees well with S_2.

An aspect which tends to support the choice of mass-based flow scales is that the range of γ is considerably smaller than that of S_1. Nevertheless, γ is close to unity for free jets and plumes [34], but up to 2.7 for the flows under consideration. This considerable range suggests that a separate model of the form $\gamma = \gamma(Ri_e^*)$ might be needed to describe the variation of γ due to the dampening effect of gravity on the transverse diffusion of buoyancy.

Table 1 Measured flow scales for katabatic winds

	H[m]	h[m]	$h_i = \gamma h$[m]	u_a[m/s]	U[m/s]	u_e[m/s]	u[m/s]
Min	47	14	49	0.6	0.6	1.4	2.3
Max	112	95	133	2.4	2.7	2.3	3.8
Mean	69	44	82	1.7	1.9	1.8	3.3
Median	67	41	78	2.0	2.1	1.8	3.5
	Δ(m/s^2)	g'(m/s^2)	$g'_i = g'/\gamma$	Ri	Ri^*	Ri_e	Ri_e^*
Min	0.02	0.07	0.05	0.19	0.2	0.7	0.8
Max	0.14	0.76	0.08	0.56	1.2	1.8	2.8
Mean	0.08	0.20	0.07	0.37	0.5	1.1	1.7
Median	0.07	0.12	0.07	0.40	0.4	0.9	1.7
	S_1	S_2	γ	β	h/H	h_i/H	u_e/U
Min	0.3	1.0	1.0	1.01	0.3	1.0	0.71
Max	1.8	1.3	2.7	1.23	0.7	1.4	0.99
Mean	0.7	1.1	1.8	1.08	0.5	1.2	0.87
Median	0.7	1.1	1.7	1.03	0.6	1.1	0.84

6 Comparison of top-hat and other scales for nonentraining flows

Width scales based on local properties of the buoyancy distribution have extensively been used for weakly entraining flows on small slopes. Examples of such local width scales are the width δ_v determined by flow visualization, the half-width of the buoyancy distribution, and the height of the maximum gradient of the density distribution [17]. For flows on a horizontal bed the term in $\sin\varphi$ in (1), and the entrainment due to gravitational forces, vanish, and a boundary layer develops at the interface between the two layers. It is then of interest to determine the relation between local and top-hat depth scales of the lower layer.

When the velocity u_l and buoyancy g'_l below the interfacial boundary layer are uniform, and the upper layer flows with a constant velocity u_a, the interface can be chosen at the height y_b at which the local buoyancy $\overline{g}'$ is $g'_l/2$. This height is generally close to the center of shear [37]. Provided that the profiles of velocity and buoyancy are symmetrical to that location it can be easily shown that the NF scales h_i, $u_{ei} = u_e$, and g'_i are the same as for a flow with a sharp interface at y_b, and a uniform distribution of velocity and density above and below that level. In contrast, the vertical extent $h = h_i/\gamma$ of the excess mass, depends on the shape of the buoyancy distribution. For a distribution according to

$$\overline{g}' = \frac{g'_l}{2}\{1 - \tanh[2(y - y_b)/\delta_b]\} \tag{22}$$

[37], where δ_b is the width of the boundary layer, the ratio $h/y_b = 1/\gamma$ is approximately

$$\frac{h}{y_b} \simeq 1 + \frac{(\pi\delta_b/y_b)^2}{48}, \quad (y_b \gg \delta_b). \tag{23}$$

For nonentraining flows h thus exceeds $h_i = y_b$, i.e. the vertical extent of the excess mass exceeds the flow depth of the lower layer. This is not a problem as long as a net entrainment of fluid through the interface at y_b is disallowed, and the shallow water equations can again be stated either in terms of mass-based or intermediate flow scales.

A special case of flows with negligible entrainment are arrested saline wedges, in which the fluxes of volume and buoyancy both vanish by definition, and for which u_a is the relevant velocity. The excess fluxes of volume and buoyancy are then $-u_a \gamma h = -u_a h_i$ and $-u_a g' h$. The excess momentum flux can be expressed in terms of a momentum coefficient β_w as $M_e = \rho u_a^2 (\beta_w - 1) h_i$. The depth h_i then corresponds to the displacement thickness, and $\beta_w h_i$ to the momentum thickness.

When the upper layer is not deep, the dynamics of the two layers can be coupled, and an interface needs to be defined. One option is to assign the interface to a location at near the center of shear, at which the velocity gradient is highest. Another one is to locate the interface near the upper edge of the buoyant shear layer to include most of the buoyancy, and to avoid the region of high shear [38,39]. Depending on the choice of the interface location, the streamwise extent of the flow, and its complexity, a shear stress is introduced at the interface.

After choosing a suitable interface, integral flow scales can be derived by carrying volume and momentum flux integrals in (1) to the height of the interface, and the momentum flux can again be accounted for by a momentum coefficient. The remaining integrals in (1) and (2) can be left unbounded to derive an integral buoyancy scale, and shape factors, in analogy to ET's approach. By choosing a depth δ as the interface height, the result is

$$\delta u_\delta = \int_0^\delta \overline{u} \mathrm{d}y, \quad \beta_\delta u_\delta^2 \delta = \int_0^\delta \overline{u}^2 \mathrm{d}y, \quad \Delta_\delta u_\delta \delta = g' h u \tag{24}$$

$$S_{1\delta} \Delta_\delta \delta^2 = g' h^2, \quad S_{2\delta} \Delta_\delta \delta = g' h, \quad Ri_\delta = \Delta_\delta \delta \cos\varphi / u_\delta^2 \tag{25}$$

The entire buoyancy is thus assigned to the lower layer, as indicated by the corresponding mass-based scales. Analogous relations can be obtained for other depth scales.

The time-averaged visual layer depth δ_v is difficult to determine when the flow is strongly entraining, and the interface unsteady [38]. Moreover, width scales like y_u and δ_v derived from local properties of the velocity and buoyancy distributions are not intimately associated with forces acting on a flow unless it is self-preserving. Considering the substantial improvement of measuring and data processing techniques in the last few decades, an alternative option is to choose width scales related to integral properties of the distributions.

An integral width scale which can be expected to be close to y_u and y_b for nonentraining flows is the interface height Y_q through which there is no net flow, i.e. below which the flow rate is equal to q_0. In arrested saline wedges the volume flux is zero by definition, and data by Sargent and Jirka [40] (their Fig. 9) show that the height Y_q, above which the entire approach flow passes, agrees closely with both the half-width y_b and the visible width δ_v of the lower layer.

A further rugged flux-delimited depth scale can be defined by considering two-layer flows as a superposition of the throughflow of velocity u_t averaged over the entire water depth, and an equal counterflow q_{ec} in the upper and lower layer [41]. The interface is then generally at the uppermost intersection where $u_t = \overline{u}$ in case a free surface without boundary shear is present. For symmetrical velocity and buoyancy distributions the interface position relative to the center of shear then depends on the depth ratio of the upper and lower layers. In particular, Y_{ec} moves upwards relative to it when the ratio increases. This can be a problem when a shear stress is to be assigned to the interface, unless the boundary layer is thin.

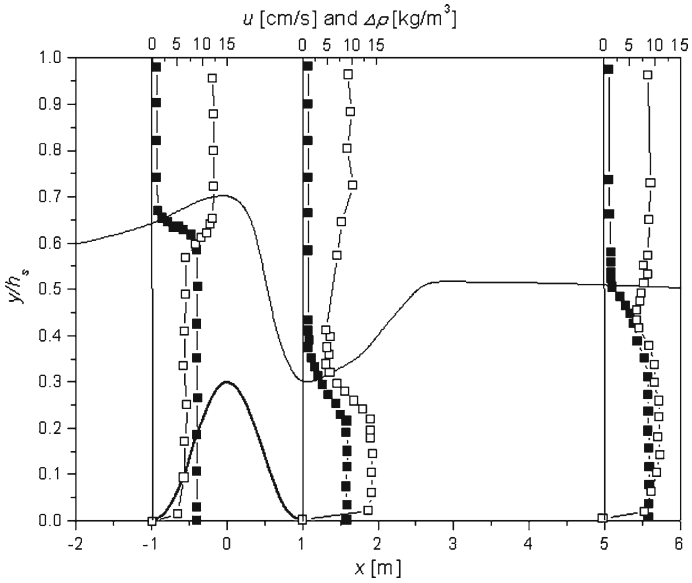

Fig. 3 Figure reproduced from Lawrence 1993 [38]. The flow is from left to right. Profiles of density difference $\Delta\rho = \rho - 1,000\,\mathrm{kg/m^3}$(■), and velocity (□), are presented at three positions along the plate ($x = -1$, 1and 5 m). The thick line presents the obstacle (hill) and the thin one presents the visual observations of the interface

To compare the mass-based scales with local scales y_b, and δ_v, as well as with the flux delimited scales Y_q and Y_{ec}, we examined the buoyancy and velocity distributions obtained by Lawrence [38] in a two-layer flow over an obstacle, as shown in Fig. 3. The flow is from left to right in both layers, density is measured in σ_t units, where $\rho(\sigma_t) = \rho(\mathrm{kg/m^3}) - 1,000$, and velocity in cm/s. The water depth h_s was 0.511 m, and the buoyancy g_0' at the source $8.8 \cdot 10^{-2}\mathrm{m/s^2}$. The flow rate q_0 was $2.05 \cdot 10^{-2}\mathrm{m^2/s}$ in the lower layer, and the total through-flow $q_t = 4.09 \cdot 10^{-2}\mathrm{m^2/s}$, resulting in a depth-averaged through-flow velocity $u_t = 80.0\,\mathrm{mm/s}$. All data were obtained from the figure to minimize the effect of reproduction errors. Lawrence ignored interfacial and boundary shear, as well as entrainment, the top-hat depths h, and γh as well as the other depth scales mentioned above are then considered to agree. Upstream of the obstacle the velocity and density distributions are approximately symmetrical to the visual interface at δ_v, marked by thin solid line, which he assumed to represent the no-flow depth Y_q. The two depths can be expected to differ downstream of the obstacle as some entrainment occurs on its downslope. Due to the presence of an internal hydraulic jump the velocity distributions in the upper layer are nonuniform at $x = 1$ m and $x = 5$ m. The shape factors β and γ in Table 2a, b were thus determined in the first profile only.

Data for the remaining width scales are listed in Table 2a, bold symbols indicate that the values were normalized by the water depth h_s. The corresponding velocities, normalized by u_t, are listed in Table 2b.

The different mass-based flow depths in Table 2a agree to within about ±7% with each other, except that Y_q is considerably higher than the other values at $x = 1$ m, δ_v at 5 m, and Y_{ec} low at 5 m. This could be due to the low velocities near the interface in both of these profiles.

Table 2 Normalized width scales (a), velocity scales (b), and other quantities (c), calculated from data in Fig. 3

Station	h	γ	y_b	δ_v	Y_q	Y_{ec}
(a)						
−1 m	0.59	1.13	0.64	0.65	0.64	0.60
1 m	0.29	–	0.30	0.30	0.41	0.27
5 m	0.44	–	0.45	0.50	0.43	0.39
	u	β	u_b	u_v	u_q	u_{ec}
(b)						
−1 m	0.74	1.06	0.80	0.83	0.75	0.77
1 m	1.28	–	1.36	1.41	1.15	1.38
5 m	1.10	–	1.14	1.11	1.22	1.23
	Ri^*	Ri_{iu}	u_h/u	Ri_h	Ri_{hu}	Ri^*_{uest}
(c)						
−1 m	6.13	0.86	1.04	5.51	1.26	1.23
1 m	0.8	–	1.09	0.63	4.21	4.11
5 m	2.31	–	1.01	2.23	3.09	3.02

When the upper layer velocity is uniform, an alternative procedure is to pack the excess fluxes of volume and momentum into the layer below γh. The corresponding value of $\gamma h/h_s$ at −1 m is 0.67 for $\gamma = 1.13$. The Richardson number $Ri^* = Ri_i$ at that location is shown in Table 2c, and the one in the upper layer is then $Ri_{iu} = g'(h_s - h_i)/(\gamma u_a^2)$. The Richardson number Ri^* can also be evaluated in the other cross-sections, where the upper layer velocity is nonuniform. To examine the corresponding velocity scales, we also located the interface at the depth h. The ratios $u_h/u = S_{1h} = S_{2h} = g'/\Delta_h$ according to (24) and (25), shown in Table 2c, indicate that the mean flow velocities u_h agree rather well with u. The Richardson number $Ri_h = \Delta_h h/u_h^2$, and the one of the upper layer $Ri_{hu} = \Delta_h(h_s - h)^3/(u_t h_s - u_h h)^2$ are included for comparison. When no velocity measurements are available, but the throughflow is known, an estimate of this Richardson number is $Ri^*_{uest} \cong g'(h_s - h)^3/(q_t - uh)^2$.

Regardless of whether a flow is self-preserving or not, and whether the water depth is large or limited, mass-based top-hat scales are thus useful for tracking the flow along its path, as they represent gravitational forces and fluxes. Similarly, measured distributions of velocity and buoyancy can be normalized with the scales g', h, and u instead of the half-widths of the velocity and buoyancy distributions when the flows are not self-preserving. Another advantage of mass-based scales compared to those of ET is that a distinction between the widths γh of the velocity distribution and h of the buoyancy field can be made when the ambient velocity is known and uniform ($\mathrm{d}u_a/\mathrm{d}x = 0$).

7 Conclusions

Gravity currents on an incline are often analyzed by using the top-hat flow scales of Ellison and Turner (ET). In a first part of the present contribution, their entrainment relation

(6) is compared with a modified version of a diffusion relation of Prandtl for jets, wakes and mixing layers (10). This relation is shown to agree with experimental data for wall jets and wall plumes ($Ri = 0$), as the widening rate D of these flows is approximately the same, but not the value of the entrainment function E. The new parameterization is applicable for forced plumes on an incline, which gradually evolve into an equilibrium gravity current. As the diffusion relation is not consistent with the continuity equation, the relation is only valid for supercritical flows on uniform topography.

Whereas the structures of ET's entrainment relation, and of their shallow water equations, are consistent with the ones for open channel flows, their flow scales are not. The reason for the difference is that the water depth is the extent of the vertical distribution of the liquid mass, whereas layer depth H of ET is based on the velocity distribution in analogy to the usual procedure for free shear flows, see (3) and (4). To reconcile the two descriptions, two mass-based sets of flow scales are outlined for gravity currents. The first set is based on the flux and distribution of buoyancy only. The velocity u is derived as the ratio of the buoyancy flux and the excess pressure at the bottom. The excess pressure force in a cross section is also required to derive a buoyancy scale g' and a depth scale h over which the buoyancy extends, see (11). The main advantage of these flow scales is that they are consistent with those which are used for open channel flows. Conversely, the depth scale H of ET can differ considerably from the water depth when it is evaluated for open channel flows, or the depth h of weakly entraining gravity currents. In cases where the buoyancy flux is known, the proposed scales can also be derived for gravity currents without measuring the velocity distribution. When the ambient velocity u_a is uniform in the transverse direction, a (generally larger) depth γh can be defined, which accommodates the excess volume flux, and u^2 is modified by a shape factor β to accommodate the excess momentum flux in (12). β is the conventional momentum, or Boussinesq, coefficient, which accounts for the non-uniformity of the velocity distribution. Errors in the velocity measurements thus affect the momentum Eq. (13) only, when the buoyancy flux is known.

An intermediate set of flow scales by Noh and Fernando [22] distinguishes only a single depth scale $h_i = \gamma h$, and the buoyancy is distributed over the entire depth, so that the buoyancy scale g_i' is g'/γ. The other quantities correspond to those of the first set, and their scales in (20) are again consistent with those of open channel flows. A similarity of their scales with those of ET is that both are based on the concept of dilution, i.e. the buoyancy scale is derived by dividing the buoyancy flux by the volume flux.

The shape factors S_1 and S_2 of ET, and the corresponding coefficients γ and β of the mass-based sets were evaluated by Altinakar [33] for his experiments with saline gravity currents on an incline. S_1 ranged from 0.48 to 1.11, γ from 1.10 to 1.86, $S_2 = \beta$ from 0.92 to 1.11. For both nonentraining gravity currents and free jets and plumes, the value of γ is slightly less than one [34]. The two sets of flow scales, as well as the shape coefficients, were also evaluated for field data on katabatic winds in a co-flow by Princevac et al. [23] (Fig. 2; Table 1). A hopeful sign is that the range of S_1 is again larger than that of γ, and that β is in the range of values for open channel flows, from about 1.03 to 1.33. S_2 again agrees well with β even though co-flows are present in the upper layer in this case.

Both ET's and mass-based scales are derived from integrals over the entire velocity and density excess distribution in the lower layer, they are also called top-hat scales. Another type of scales, which have often been used, is based on local properties of the buoyancy or velocity distribution. Examples are the buoyancy half-width or the layer width determined by flow visualization. In contrast to top-hat scales these scales are not directly related to forces, unless the flows are self-preserving, and the shape of the distributions of velocity and buoyancy known. A third type of flux-delimited width scales can be defined, which depend

on both integral and local properties of the flow. These two types of scales are compared with mass-based ones for a rather rapidly varying two-layer flow over an obstacle (Fig. 3; Table 2). The different width scales agree reasonably well with each other. Depending on whether the upper layer velocity is uniform or not, fully mass-based and intermediate flow scales again have definite advantages over the local and flux delimited ones.

Fully mass-based and intermediate flow scales represent gravity forces acting on the flow, and fluxes. They are thus a good measure for comparisons of experimental data at different cross-sections of a flow, regardless whether the flow is self-preserving or not, whether the ambient flow is uniform or not, and whether the water is deep or of limited depth. Similarly, buoyancy and velocity distributions can conveniently be made nondimensional in terms of fully mass-based or intermediate flow scales.

Acknowledgements The initial motivation for this study arose during a sabbatical of the second author in Lausanne, for which he expresses his gratitude to Dr. Schleiss.

References

1. Prandtl L (1926) Ueber die ausgebildete Turbulenz. In: Proc. 2nd int. congr. for appl. mech., Sept. 12–17, Zurich, pp 62–74
2. Schlichting H (1955) Boundary layer theory. McGraw-Hill, New York, p 535
3. Abramovich GN (1963) The theory of turbulent jets. MIT Press, Cambridge
4. Patel RP (1971) Turbulent jets and wall jets in uniform streaming flow. Aeronaut Quart XXII:311–326
5. Morton BR, Taylor GI, Turner JS (1956) Turbulent gravitational convection from maintained and instantaneous sources. Proc R Soc Lond A234:1–23
6. List EJ, Imberger J (1973) Turbulent entrainment in buoyant jets. J Hydraul Div ASCE 99:1461–1474
7. Turner JS (1986) Turbulent entrainment: the development of the entrainment assumption, and its application to geophysical flows. J Fluid Mech 173:431–471. doi:10.1017/S0022112086001222
8. Hunt JCR, Eames I, Westerweel J (2006) Mechanics of inhomogeneous turbulence and interfacial layers. J Fluid Mech 554:499–519. doi:10.1017/S002211200600944X
9. Bühler J, Princevac M, Schleiss A (2008) Widening rates of forced plumes on an incline. In: Proc 2nd int symposium on shallow flows, Dec. 10–12, Hong Kong (to be published)
10. Bühler J, Papantoniou DA (2001) On the motion of suspension thermals and particle swarms. J Hydraul Res 39(6):643–653
11. Lee JHW, Chu VH (2003) Turbulent jets and plumes: a Lagrangian approach. Kluwer, Dordrecht
12. Ellison TH, Turner JS (1959) Turbulent entrainment in stratified flows. J Fluid Mech 6:423–448. doi:10.1017/S0022112059000738
13. Parker G, Garcia M, Fukushima Y, Yu W (1987) Experiments on turbidity currents over an erodible bed. J Hydraul Res 25(1):123–146
14. Alavian V, Jirka GH, Denton RA, Johnson MC, Stefan HG (1992) Density currents entering lakes and reservoirs. J Hydraul Eng 118(11):1464–1489. doi:10.1061/(ASCE)0733-9429(1992)118:11(1464)
15. Altinakar MS, Graf WH, Hopfinger EJ (1996) Flow structure in turbidity currents. J Hydraul Res 34(5):713–718
16. Bühler J, Siegenthaler C (1986) Self-preserving solutions for turbidity currents. Acta Mech 63(11):217–233. doi:10.1007/BF01182549
17. Fernandez RL, Imberger J (2006) Bed roughness induced entrainment in a high Richardson number underflow. J Hydraul Res 44(6):725–738
18. Manins PC, Sawford BL (1979) A model of katabatic winds. J Atmos Sci 36:619–630. doi: 10.1175/1520-0469(1979)036<0619:AMOKW>2.0.CO;2
19. De Cesare G, Boillat J-L, Schleiss A (2006) Circulation in stratified lakes due to flood-induced turbidity currents. J Environ Eng 132(11):1508–1517.doi:10.1061/(ASCE)0733-9372(2006)132:11(1508)
20. Oehy CD, Schleiss AJ (2007) Control of turbidity currents in reservoirs by solid and permeable obstacles. J Hydraul Eng 133(6):637–648. doi:10.1061/(ASCE)0733-9429(2007)133:6(637)
21. Buhler J, Schlaepfer DB (1986) New width and other scales for entraining shear flows. In: Proc int symp on buoyant flows, Athens, pp 37–46

22. Noh Y, Fernando HJS (1991) Gravity current propagation along an incline in the presence of boundary mixing. J Geophys Res 96(C7):12586–12592. doi:10.1029/90JC02488
23. Princevac M, Fernando HJS, Whiteman D (2005) Turbulent entrainment into natural gravity-driven flows. J Fluid Mech 533:259–268. doi:10.1017/S0022112005004441
24. Wright SJ (1994) The effect of ambient turbulence on jet mixing. In: Recent research advances in the fluid mechanics of turbulent jets and plumes, NATO ASI series, Kluwer, Dordrecht, pp 13–27
25. Townsend AA (1956) The structure of turbulent shear flow. Cambridge University Press, Cambridge
26. Grella JJ, Faeth GM (1975) Measurements in a two-dimensional thermal plume along a vertical adiabatic wall. J Fluid Mech 71(4):701–710. doi:10.1017/S0022112075002807
27. Boussinesq JV (1877) Essai sur la théorie des eaux courantes (On the theory of flowing waters). Mémoires présentés par divers savants à l'Académie des Sciences, 23, Paris
28. Escudier MP, Maxworthy T (1973) On the motion of turbulent thermals. J Fluid Mech 61:541. doi:10.1017/S0022112073000856
29. Chow V-T (1959) Open channel hydraulics. McGraw Hill, New York
30. Bühler J (1983) On integral scales for jetlike flows. In: 8th Australian fluid mech conf, vol 2, Newcastle, Australia, 8.9-8C.12
31. Bühler J, Wright SJ, Kim Y (1991) Gravity currents advancing into a coflowing fluid. J Hydraul Res 29(2):243–257
32. Taylor G (1958) Flow induced by jets. J Aeronaut Sci 25(1):464–465
33. Altinakar MS (1993) Weakly depositing turbidity currents on small slopes. PhD thesis nr. 738, Dept. of Civil Engineering, Ecole Polytechnique Fédérale de Lausanne (EPFL), Lausanne, Switzerland
34. Bühler J, Princevac M (2007) A common depth scale for gravity currents and open channel flow. In: Proc 32nd IAHR congress, Venice, CD-Rom, C1.a-002
35. Wood IR (1983) Uniform region of self-aerated flows. J Hydrol Eng 109(3):447–461
36. Doran JC, Fast JD, Horel J (2002) The VTMX 2000 campaign. Bull Am Meteorol Soc 83(4):537–554. doi: 10.1175/1520-0477(2002)083<0537:TVC>2.3.CO;2
37. Dermissis V (1990) Velocity distribution in arrested saline wedges. Waterway Port Coast Ocean Eng 116(1):21–42. doi:10.1061/(ASCE)0733-950X(1990)116:1(21)
38. Lawrence GL (1993) The hydraulics of two-layer flow over a fixed obstacle. J Fluid Mech 254:605–663. doi:10.1017/S0022112093002277
39. Hogg AJ, Hallworth MA, Huppert HE (2005) On gravity currents driven by constant fluxes of saline and particle-laden fluid in the presence of a uniform flow. J Fluid Mech 549:349–385. doi:10.1017/S002211200500546X
40. Sargent FE, Jirka GH (1987) Experiments on saline wedge. J Hydraul Eng 113(10):1307–1324
41. Bühler J (1994) Simple internal waves and bores. J Hydraul Eng 120(5):638–645